

DESIGN AND WINDTUNNEL TESTS OF AN AIRFOIL FOR THE HORIZONTAL TAILPLANE OF A STANDARD CLASS SAILPLANE

By L.M.M. Boermans and F. Bennis
of the Delft University of Technology, The Netherlands

Presented at the XXII OSTIV Congress, Uvalde, Texas, U.S.A. (1991)

INTRODUCTION

The horizontal tailplane of a sailplane operates at low Reynolds numbers, typically from $Re = 0.5 \cdot 10^6$ to $1.5 \cdot 10^6$, where laminar separation bubbles play a detrimental role. To avoid these bubbles, Wortmann applied extensive instability regions on his well-known tailplane airfoils FX71-L-150/20, /25 and /30 (Reference 1). The success of artificial transition control on modern sailplane wings — thus avoiding bubbles and making longer laminar flow regions possible — is the obvious reason to apply this technique, also in designing a

new airfoil for the horizontal tailplane of the Standard Class sailplane ASW-24, produced by Alexander Schleicher Segelflugzeugbau, Germany. It is evident that the airfoil is useful for any sailplane tailplane application provided similar operating conditions.

In the next chapters, a specification of desirable tailplane airfoil characteristics is drawn up, a new airfoil design is described, and windtunnel test results are presented.

REQUIREMENTS

The operational variation of angles of attack and elevator deflections in straight and circling flight at forward and aft c.g. positions was calculated with the method of Reference 2. As shown in Figure 1, the tailplane angle of attack at a certain wing lift coefficient in straight flight is independent of the c.g. position, and increases in circling flight, depending on the angle of bank. The wing loading only affects this angle of attack increase; the largest increase is obtained at the lowest wing loading (used in Figure 1). It is noted that the maximum wing lift coefficient is 1.3, and the lower boundary of the low drag bucket is at a wing lift coefficient of 0.25.

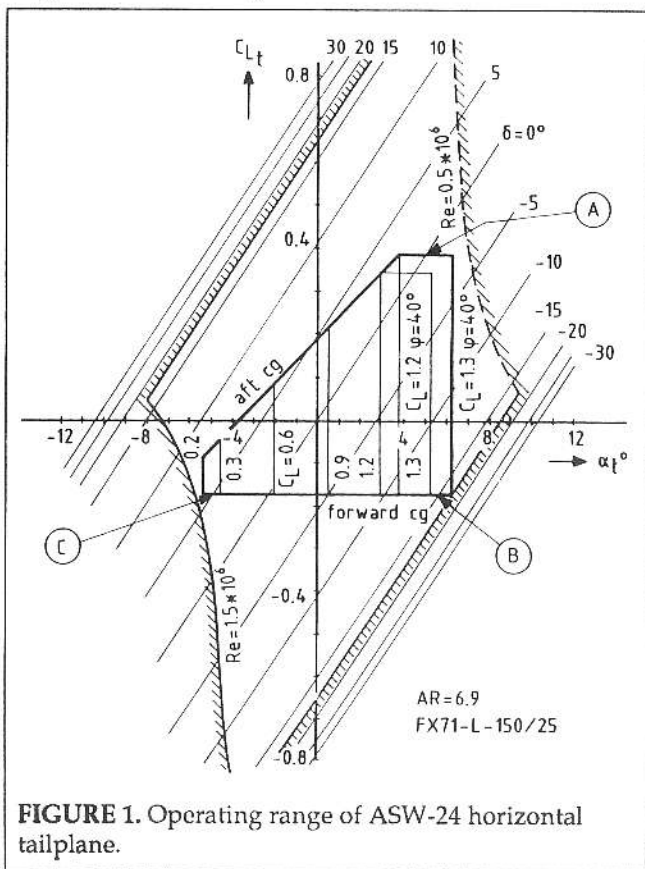


FIGURE 1. Operating range of ASW-24 horizontal tailplane.

To illustrate the conditions A, B, and C, which are relevant for the airfoil design process, the lift characteristics and estimated low drag boundaries of airfoil FX71-L-150/25 are overlaid in Figure 1, and at corresponding lift coefficients (for simplicity), calculated potential flow velocity distributions and transition points as well as measured airfoil drag characteristics (not available at $Re = 0.5 \times 10^6$) are shown in Figure 2.

Condition A: The elevator angle is about zero degrees and the airfoil operates near the upper boundary of the low drag bucket.

Taking into account that the local lift coefficient on the actual ASW-24 tailplane is at most 9% higher than the total lift coefficient, the upper boundary of the low drag bucket should be at $c_l = 0.45$ at $Re = 0.5 \times 10^6$ and $\delta = 0$ degrees. In addition, the drag increase beyond the low drag bucket should be gradual because excursions beyond the low drag bucket are easily made in thermaling flight conditions.

Condition B: The tailplane operates at the same positive angle of attack as in condition A, but the elevator angle is about -15 degrees. The upper boundary of the low drag

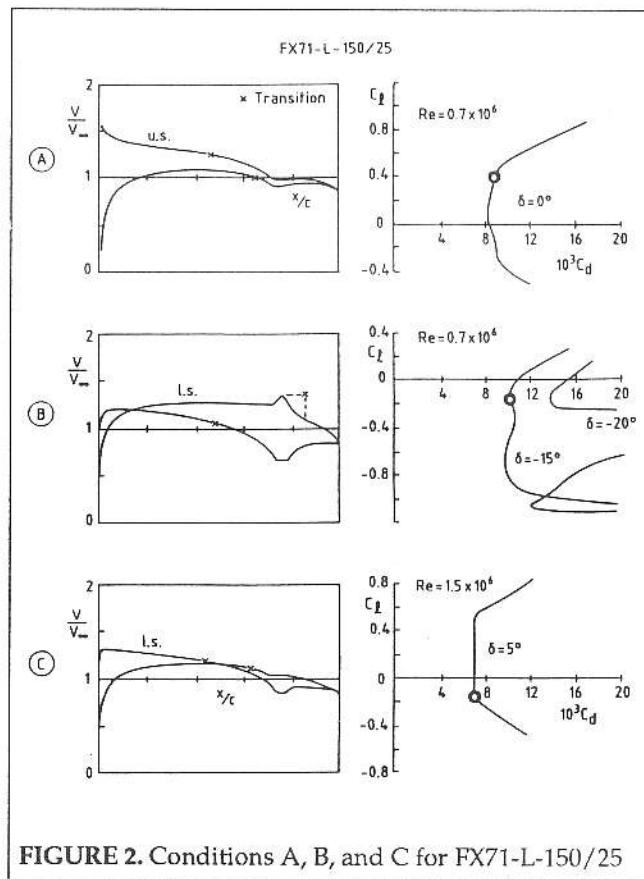


FIGURE 2. Conditions A, B, and C for FX71-L-150/25

bucket is relevant again. Besides, due to the formation of a laminar separation bubble on the lower elevator surface, the drag may increase drastically, as illustrated by the characteristics at $\delta = -20^\circ$. Artificial transition by a turbulator in front of the flap would be beneficial.

Condition C: The tailplane operates at a negative angle of attack, and a positive elevator angle of about 5 degrees.

Here, the lower boundary of the low drag bucket at $Re = 1.5 \times 10^6$ is relevant. This lower boundary should be at $c_l = 0.2$ at $Re = 1.5 \times 10^6$ and $\delta = 5$ degrees.

In addition to these drag characteristics, $c_{l,max}$ values are required to be comparable to the values of the Wortmann tailplane airfoil. This requirement is set on safety grounds, in particular to counteract undesired motions of the airplane, due to stationary cable towing at the beginning of the launch.

Finally, in order to obtain stick forces meeting the airworthiness requirements, it is customary to extend the flat elevator upper surface of the Wortmann airfoil a few percent, thus producing a hinge moment acting in the flap-up direction. This feature should be implemented in a new tailplane airfoil design.

Airfoil Design

Given the previously discussed requirements, a new airfoil was designed with the airfoil analysis and design computer code developed at the Low Speed Windtunnel Laboratory of the Delft University of Technology, Faculty of Aerospace Engineering, Reference 3. Experience with this code was gained during the design, analysis and experimental verification of several airfoils for sailplane application, References 4 and 5.

Figure 3 shows the airfoil, named DU86-137/25, and some

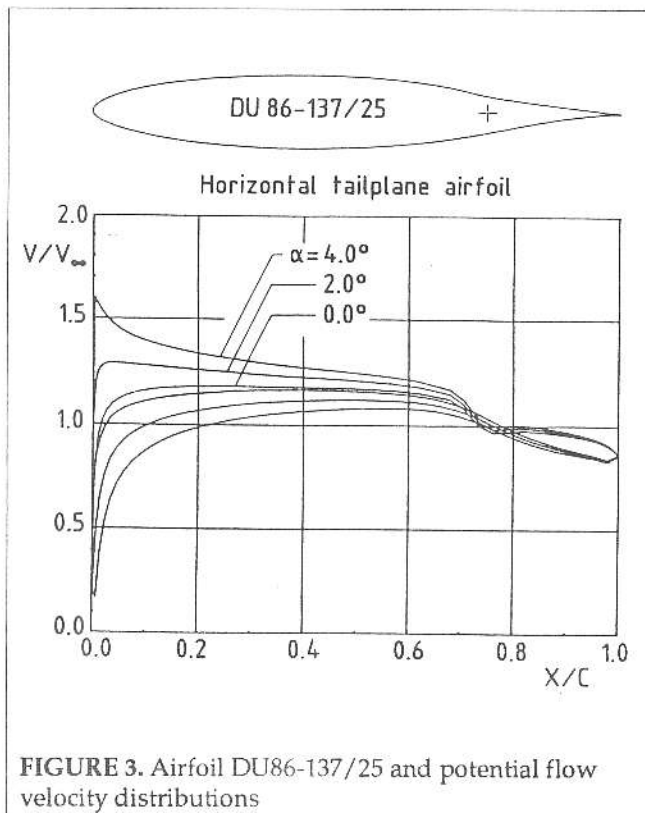


FIGURE 3. Airfoil DU86-137/25 and potential flow velocity distributions

potential flow velocity distributions. The coordinates with 0 degree flap deflection are presented in Table 1. The airfoil is asymmetrical, has a relative thickness of 13.7% chord and a flap of 25% chord.

The upper surface pressure distribution was designed to avoid a steep adverse pressure gradient on the flap at positive flap deflections. The pronounced laminar separation bubble,

which will appear owing to the steep pressure gradient at 70% chord has to be eliminated by artificial means. The flat upper flap surface helps in creating a turbulent boundary layer form parameter, which development, at high angles of attack, is similar to the Wortmann airfoil mentioned before; therefore, $c_{l,max}$ was expected to be about the same.

Usually, high performance sailplanes have a T-tail configuration where the leading edge of the horizontal tailplane midspan section projects in front of the vertical tailplane. As a result, the laminar boundary layer on the lower surface of the horizontal tailplane turns turbulent and separates as it approaches the vertical tailplane stagnation point, and the separated flow is observed at the rear part of the corner, Reference 6. In order to improve the flow conditions at the junction, a steep adverse pressure gradient was not applied on the lower surface of the airfoil (and the leading edges of the ASW-24 horizontal and vertical airfoil coincide). Nevertheless, artificial transition control has to be applied on the lower surface too, to avoid laminar separation bubbles behind the flap hinge, in particular at combinations of positive angles of attack and negative flap angles.

Finally, as a by-product of the different pressure distributions on the flap upper and lower surface, some amount of hinge moment is present which acts in the desired direction.

WINDTUNNEL TESTS

Windtunnel, model, instrumentation, data reduction

The Low-Speed Low-Turbulence Windtunnel of Delft University of Technology, Faculty of Aerospace Engineering, is of the closed return type. It has a contraction ratio of 17 and an interchangeable octagonal test section of 1.80 m wide and 1.25 m high. The turbulence level in the test section varies from 0.018% at 10 m/s to 0.043% at 60 m/s.

The windtunnel model, being half of the ASW-24 horizontal tailplane, was built in the actual production mould at Alexander Schleicher Segelflugzeugbau and provided with 94 pressure orifices (diameter 0.4 mm), located in eight

TABLE 1. Co-ordinates of DU 86-137/25

UPPER SURFACE							
x/c	y/c	x/c	y/c	x/c	y/c	x/c	y/c
%	%	%	%	%	%	%	%
0.007	0.131	4.774	3.218	30.155	6.697	65.012	5.168
0.138	0.578	7.677	4.039	35.786	6.844	70.506	4.177
0.453	1.015	11.186	4.791	41.606	6.846	76.229	2.984
0.964	1.457	15.249	5.448	44.559	6.790	81.686	2.223
1.656	1.904	19.809	5.992	50.494	6.558	90.745	1.084
2.524	2.349	29.803	6.411	59.305	5.881	100	0
LOWER SURFACE							
x/c	y/c	x/c	y/c	x/c	y/c	x/c	y/c
%	%	%	%	%	%	%	%
0.047	-0.301	4.516	-2.770	24.533	-6.151	61.773	-5.691
0.294	-0.696	7.410	-3.583	29.857	-6.517	70.167	-4.506
0.764	-1.091	10.924	-4.348	35.450	-6.736	80.775	-2.457
1.435	-1.052	14.994	-5.048	41.232	-6.799	90.121	-0.862

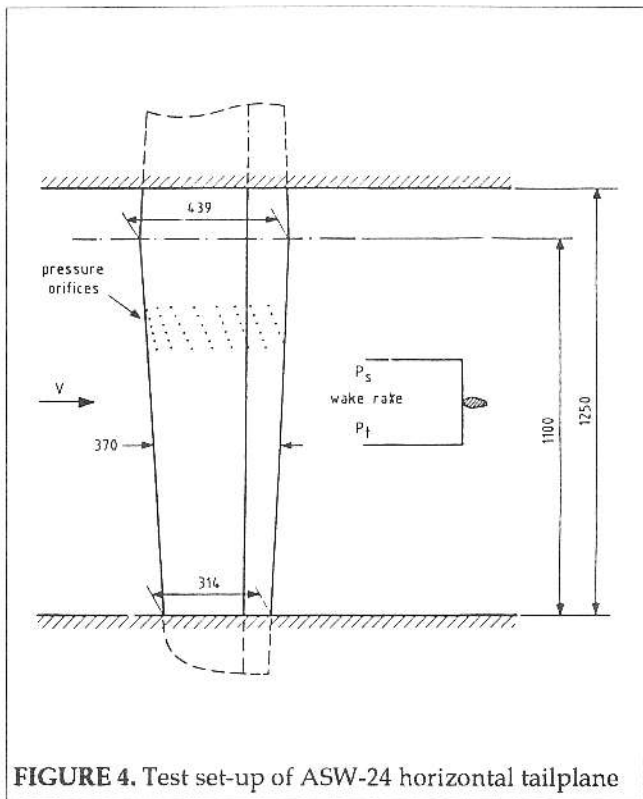


FIGURE 4. Test set-up of ASW-24 horizontal tailplane

oblique rows on the upper and lower surface, Figure 4. The model was mounted vertically between circular turntables which are flush with the upper and lower windtunnel wall. The airfoil deviates from the design at the trailing edge in what the upper surface was slightly extended (about 2.5%*c*) in order to increase the flap hinge moment as described before. This was the result of previous flight tests where the provisionally extended trailing edge was cut step by step.

A total pressure and static pressure wake rake, mounted on a cross-beam, were positioned about 66% of the local chord downstream from the model trailing edge. The wake rake

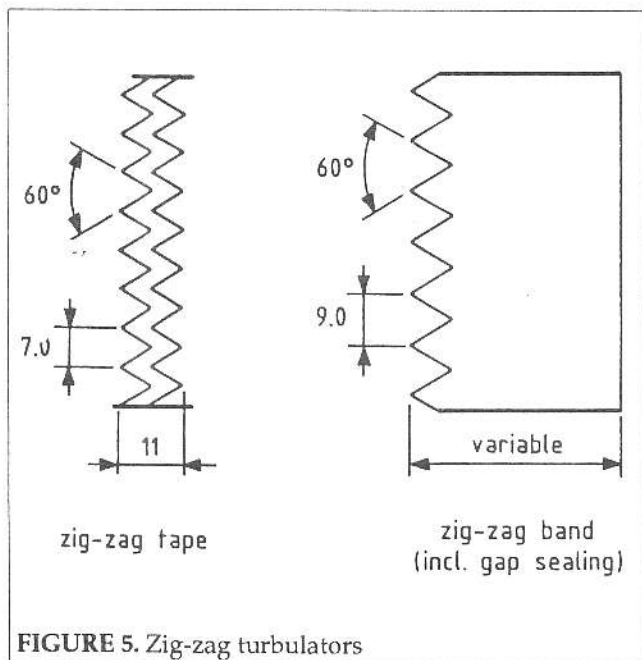


FIGURE 5. Zig-zag turbulators

employed 50 total-pressure tubes and 12 static-pressure tubes, all 1.5 mm in diameter. A pitot static tube was mounted on the tunnel sidewall.

All pressures were recorded by an automatically reading 200 tube liquid manometer and on line reduced to standard pressure coefficients. Numerical integration of the static pressure coefficients at the model surface yielded the section normal force and pitching moment coefficients. Section profile-drag coefficients were computed from the wake pressures by the method of Jones, Reference 7. Section lift coefficients were computed from the relation $c_l = c_n / \cos \alpha - c_d \tan \alpha$.

Standard low-speed windtunnel boundary corrections, Reference 8, a maximum of about 3% of the measured section characteristics and 0.2° angle of attack, have been applied to the data.

TEST RESULTS

The tests were performed at various practical combinations of Reynolds number, angle of attack and flap deflection, both with a smooth surface (free transition) and with turbulators on upper and lower surface. The turbulators consisted of zig-zag tape or zig-zags in the front of elastic bands which seal the flap gap, Figure 5.

Generally, in evaluating the drag data it should be realized that the contribution of the horizontal tailplane to the total

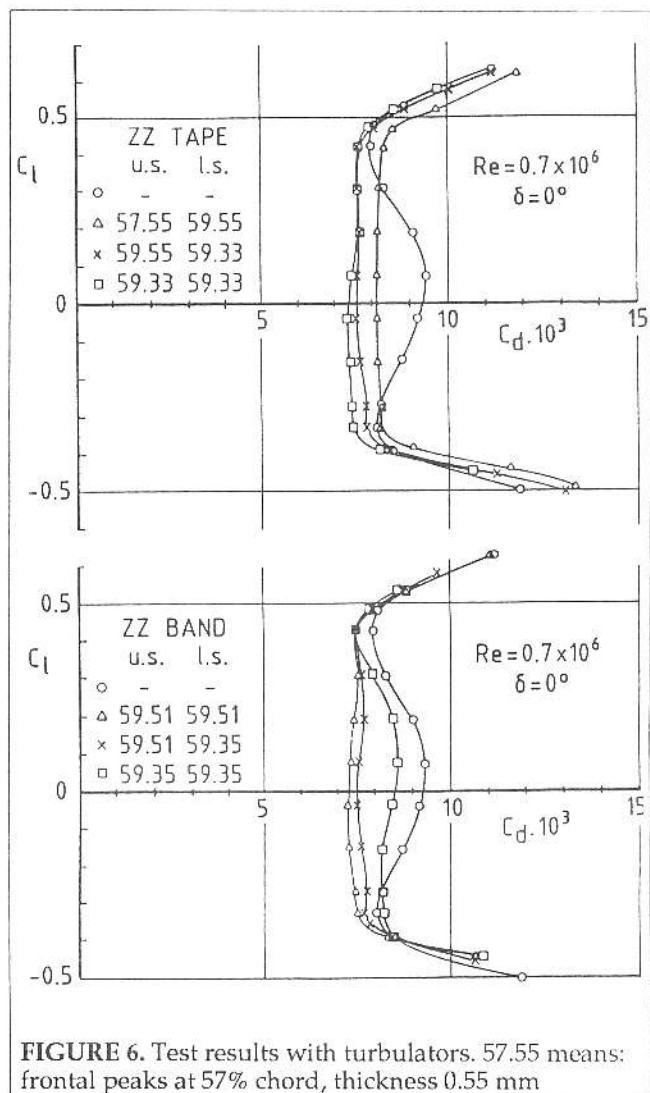
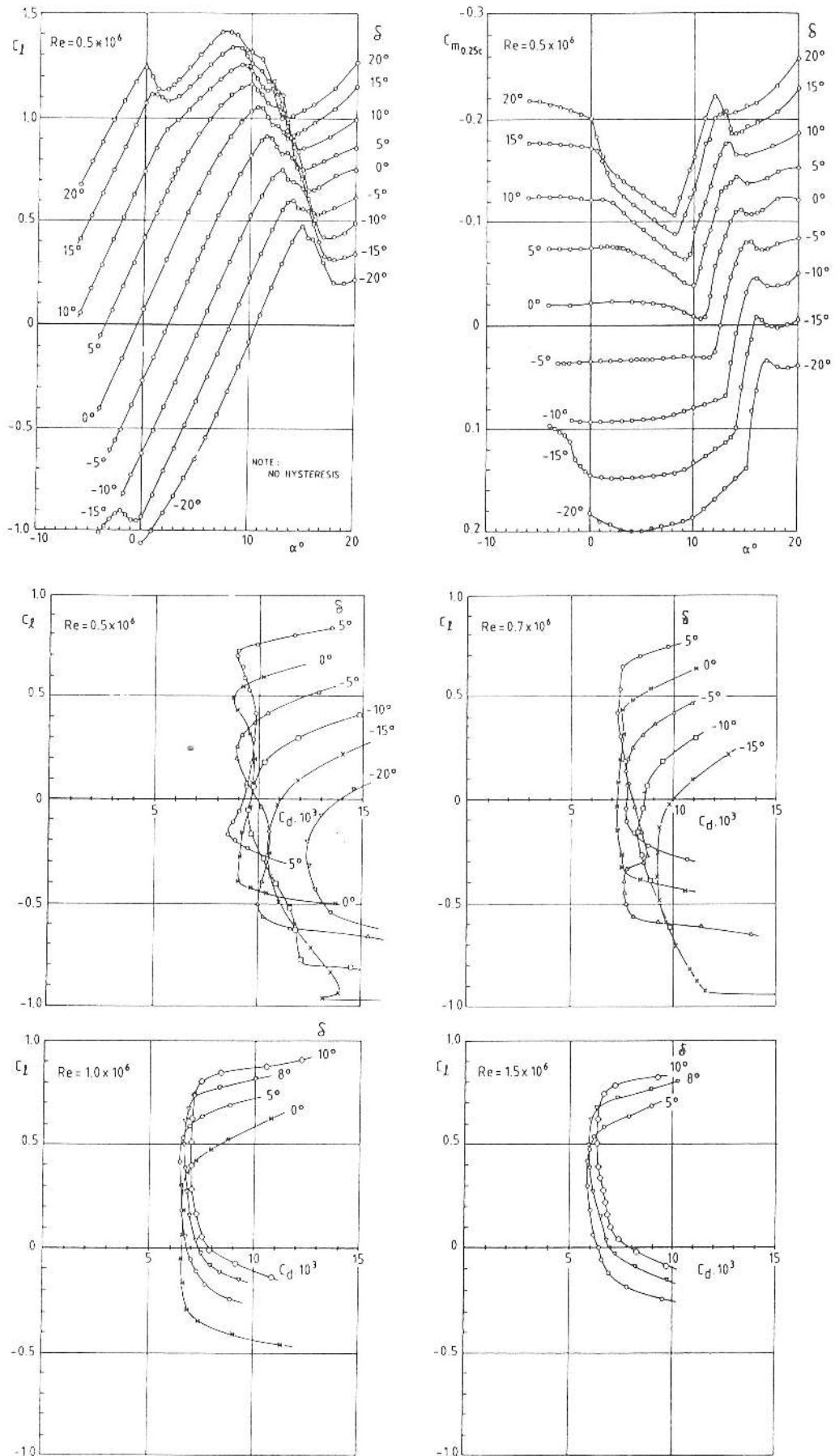


FIGURE 6. Test results with turbulators. 57.55 means: frontal peaks at 57% chord, thickness 0.55 mm

FIGURE 7. Characteristics of DU86-137/25 with zig-zag bands at practical Reynolds numbers and flap deflections.



drag and rate of sink of the sailplane amounts to about 3% at $C_L = 1$ and 6.5% at $C_L = 0.3$. A tail profile drag coefficient reduction of say 0.001 diminishes the rate of sink only about 2 mm/sec at low flight speed ($C_L = 1$) but 1.5 cm/sec at high flight speed ($C_L = 0.3$).

At first, systematic tests were performed at several practical combinations of flap deflection and Reynolds number with zig-zag tape of thickness 0.55, 0.45 and 0.33 mm at a frontal peak position between 57% and 65% chord. The flap gaps were sealed with thin tape (0.04 mm). An example of these tests is shown in the upper part of Figure 6. Overall, the best performance was measured with a 0.33 mm thick zig-zag tape at a frontal peak position of 59% c on both sides.

Then, tests were performed with elastic bands with zig-zags in the front of 0.35 or 0.51 mm thickness at a frontal peak position of 59% c. Now, the thinner zig-zags were less effective than the thicker ones as shown in the lower part of Figure 6. Obviously, the backward facing peaks of the zig-zag tape contribute to the effectiveness.

All characteristics, shown in Figure 7, were measured with elastic bands with zig-zags of 0.51 mm thickness at a frontal peak position of 59% c on upper and lower surface. Generally, these results are equivalent or slightly better than the results measured with the 0.33 mm zig-zag tape at 59% c.

The dents in the drag characteristics at $Re = 0.5 * 10^6$ indicate that laminar separation bubbles are not eliminated entirely at this low Reynolds number. This was accepted in view of the negligible effect on the rate of sink at low flight speeds, and alternatively, in view of the increase in rate of sink at high flight speeds if thicker zig-zags are applied to eliminate the bubble at $Re = 0.5 * 10^6$.

In comparison to the data of FX71-L-150/25, the minimum drag values of the new airfoil are 10%, 8% and 13% lower at respectively $Re = 0.7 * 10^6$, $1 * 10^6$ and $1.5 * 10^6$, thus an average drag reduction of about 10% was realized. The maximum lift coefficient at $Re = 0.5 * 10^6$ is estimated to be only 5% lower than the maximum lift coefficient of the (thicker) Wortmann airfoil.

CONCLUSION

Requirements, design and windtunnel tests results of a

new airfoil for application in the horizontal tailplane of the Standard Class high performance sailplane ASW-24 have been presented. The airfoil was designed for application of artificial transition. Tests showed that the functions of a flexible flap gap sealing and a zig-zag turbulator can be integrated by cutting zig-zags in the front of the sealings stuck to the surface. With zig-zags of 0.5 mm nominal thickness and frontal peaks at 59% chord on upper and lower surface, the minimum drag of the new airfoil is about 10% lower and $C_{L,max}$ only 5% lower than the well-known tailplane airfoil FX71-L-150/25. Both test flights and actual practice with the ASW-24 have shown that the airfoil behaves very well, with ample reserve in difficult situations.

REFERENCES

1. D. Althaus, Stuttgarter Profilkatalog I, Universitat Stuttgart, 1972.
2. G. Stich, Das gedampfte Hohenleitwerk in Kreisflug, OSTIV Publication XVI, 1981.
3. J.L. van Ingen, L.M.M. Boermans, Aerodynamics at low Reynolds numbers: A review of theoretical and experimental research at Delft University of Technology, Proc. of Int. Conf. on Aerodynamics at Low Reynolds Numbers, paper 1, R.A.E.S. London, 1986.
4. L.M.M. Boermans, H.J.W. Selen, Design and tests of airfoils for sailplanes with an application to the ASW-19B, ICAS-paper 82-5.5.2, 1982.
5. L.M.M. Boermans, G. Waibel, Aerodynamic and structural design of the Standard Class sailplane ASW-24, ICAS-paper 88-2.7.2, 1988.
6. L. Lautanala, Flow visualization in the horizontal and vertical stabilizer joint area of a glider aircraft. Bericht Idaflieg Wintertagung, Heft VIII, 1982.
7. B.M. Jones, Measurement of profile drag by the pitot-traverse method. R&M no. 1688, Brit. A.R.C., 1936.
8. H.J. Allen, W.G. Vincenti, Wall interference in a two-dimensional flow windtunnel with consideration of the effect of compressibility. NACA report 782, 1944.